ARMY RESEARCH LABORATORY

Conceptual Design, Engineering Modeling, and Experimental Validation of Air Sampling System for Chemical Sensor Insertion Into the U.S. Army Research Laboratory's (ARL) Silent Operating Aerial Reconnaissance (SOAR) Program

by Michael L. Nair

ARL-TR-3105 **February 2004**

NOTICES

Disclaimers

The findings in this report are not to be construed as an official Department of the Army position unless so designated by other authorized documents.

Citation of manufacturer's or trade names does not constitute an official endorsement or approval of the use thereof.

DESTRUCTION NOTICE—Destroy this report when it is no longer needed. Do not return it to the originator.

Army Research Laboratory
Aberdeen Proving Ground, MD 21005-5069

ARL-TR-3105 **February 2004**

Conceptual Design, Engineering Modeling, and Experimental Validation of Air Sampling System for Chemical Sensor Insertion Into the U.S. Army Research Laboratory's (ARL) Silent Operating Aerial Reconnaissance (SOAR) Program

Michael L. Nair
Weapons and Materials Research Directorate, ARL

REPORT DOCUMENTATION PAGE

Form Approved
OMB No. 0704-0188

1. REPORT DATE *(DD-MM-YYYY)*	2. REPORT TYPE	3. DATES COVERED (From - To)
February 2004	Final	January 2003 to May 2003

4. TITLE AND SUBTITLE

Conceptual Design, Engineering Modeling, and Experimental Validation of Air Sampling System for Chemical Sensor Insertion into the U.S. Army Research Laboratory's (ARL) Silent Operating Aerial Reconnaissance (SOAR) Program

5a. CONTRACT NUMBER

5b. GRANT NUMBER

5c. PROGRAM ELEMENT NUMBER

6. AUTHOR(S)

Michael L. Nair (ARL)

5d. PROJECT NUMBER

1L162618H80

5e. TASK NUMBER

5f. WORK UNIT NUMBER

7. PERFORMING ORGANIZATION NAME(S) AND ADDRESS(ES)

U.S. Army Research Laboratory
Weapons and Materials Research Directorate
Aberdeen Proving Ground, MD 21005-5069

8. PERFORMING ORGANIZATION REPORT NUMBER

ARL-TR-3105

9. SPONSORING/MONITORING AGENCY NAME(S) AND ADDRESS(ES)

10. SPONSOR/MONITOR'S ACRONYM(S)

11. SPONSOR/MONITOR'S REPORT NUMBER(S)

12. DISTRIBUTION/AVAILABILITY STATEMENT

Approved for public release; distribution is unlimited.

13. SUPPLEMENTARY NOTES

14. ABSTRACT

The U.S. Army Research Laboratory is interested in using a concept unmanned aerial vehicle (UAV) as a chemical weapons detection platform. This report details a preliminary effort to determine whether the UAV is capable of sustaining the needed air flow into a chemical weapons detector to ensure functionality.

For this study, it was decided that a minimum volumetric flow rate of 1.4 liters/minute is required to satisfy the minimum flow requirement. Basic fluid mechanic equations are used to select the incompressible model for air flow, and then ADINA (automatic dynamic incremental nonlinear analysis) is used to create finite element analysis approximations of the flow problem. Based on the results of the computer analysis, it was decided that the best concept for acquiring the air flow is to use a small blower with an intake and exhaust orifice in the bottom of the UAV. A prototype device has been built and tested through the estimated flight profile of the UAV.

It was found that this simple device leads to volumetric flow rates approximately 10 times higher than the minimum required for chemical weapons detection. Based on these results, it is possible to use this UAV as a chemical weapons detector with the induced air flow concept.

15. SUBJECT TERMS

chemical weapons detection; chemical weapons detector; UAV; unmanned aerial vehicle

16. SECURITY CLASSIFICATION OF:			17. LIMITATION OF ABSTRACT	18. NUMBER OF PAGES	19a. NAME OF RESPONSIBLE PERSON
a. REPORT	b. ABSTRACT	c. THIS PAGE			Michael L. Nair
UNCLASSIFIED	UNCLASSIFIED	UNCLASSIFIED	UL	45	19b. TELEPHONE NUMBER (*Include area code*) 410-306-1051

Standard Form 298 (Rev. 8/98)
Prescribed by ANSI Std. Z39.18

Contents

List of Figures

List of Tables

Acknowledgments

The author would like to thank Dave Lyon, Timothy Vong, Gordon Brown, John Condon, and Marshall Childers of the U.S. Army Research Laboratory for their support and assistance in providing the opportunity to work on this project. Special thanks to Professor Ernesto Blanco of the Massachusetts Institute of Technology (MIT) for his support and guidance throughout this project, Steve Haberek of MIT for his assistance in machining, and Dr. Barbara Hughey of MIT for the use of her lab equipment. The author would also like to thank Brian Pharris for assisting during experimentation, and Michelle Neil for her help in performing the data analysis.

INTENTIONALLY LEFT BLANK.

1. Introduction

For the past several years, the U.S. Army Research Laboratory (ARL) has been developing a concept unmanned aerial vehicle called the gun-launched unmanned aerial vehicle (GLUAV), shown in figure 1. The GLUAV is deployed from a specially designed canister inserted within a large caliber 105-mm munition that is fired from a mortar or artillery weapon system.

Figure 1. Deployed GLUAV in flight (artist's conception) from ARL-CR-515.

Upon reaching the apogee of the projectile flight path, the GLUAV is expelled and pulled from the rear of the canister by means of parachute; it then unfolds its wings and tail fins. The parachute is released from the GLUAV and free flight begins.

The GLUAV is much smaller than typical UAVs in military inventory, such as the Predator or Global Hawk. The GLUAV is approximately 25 centimeters long with a wing span of similar size. Because of the GLUAV's small size, its payload capacities are much more limited than other such vehicles. As with other UAVs, the GLUAV was originally conceived as a

reconnaissance platform to carry such equipment as video cameras and transmit the imagery back to the operator.

ARL is now considering the possibility of using the GLUAV as a platform for chemical weapons detection. In order to function as a chemical weapons detector platform, the GLUAV must be able to successfully carry the sensor as well as satisfy the operational characteristics of a chemical weapons detector.

Chemical weapons detectors function by passing air over a sensing element. This sensing element can vary in type, depending on the version and capability of the detector. However, all detectors do require a steady flow of air to sample. There is currently no chemical weapons detector of which the author is aware that will meet the design criteria for installation in the GLUAV. While size and weight are certainly limiting factors, the most challenging factor for this application is the survivability of the sensor. As the GLUAV is gun launched, it can undergo an initial "set-back" acceleration of approximately 15,000 times the force of gravity upon propellant ignition and then experiences an acceleration in the opposite direction ("set forward") of about 10% to 50% (50% being the worst case) of that level as it travels down the gun barrel. These forces require a sensor that has been specifically designed to survive such loads, usually by the encapsulation of sensitive components. Since this analysis is a first-level study to determine the feasibility of using chemical weapons detectors, no work has been conducted in designing a detector for this particular application with its unique operational requirements. However, if testing is successful and ARL decides to proceed with development, a sensor will be designed and tested to meet the requirements for use in the GLUAV. Since weight and size of the detector will be determined when a sensor is designed, the critical parameter for the functionality of a chemical weapons detector for the GLUAV is the sustainability of sufficient air flow to the sensing element.

To determine the air flow requirements for chemical weapons detectors, three sources were contacted. Environics[1], a company based in Finland, produces a small hand-held chemical weapons detector called the ChemPro100, which requires a steady flow of 1 liter per minute (L/min) of air. BAE Systems[2] has recently developed the Chemsonde detector (see http://www.nbcindustrygroup.com/baesys.htm), a self-contained sensor designed to be packaged in a MJU-10 military flare cartridge. The Chemsonde system requires an air flow of only 0.1 L/min according to information provided to ARL by BAE Systems. Finally, the U.S. Army Soldier and Biological Chemical Command (SBCCOM) was contacted about their experience with detectors. They reported that typical military sensors require an air flow of 1.2 to 1.4 L/min to function adequately. The correspondence with SBCCOM and Environics is presented in appendix A. Since there is some variance in the information reported, it will be assumed that greater air flow than 1.4 L/min will be sufficient for chemical weapons detection.

[1]Environics OY, Graanintie 5, P.O. Box 349, FIN-50101 Mikkeli, Finland.

[2]BAE Systems, Integrated Defense Solutions, 6500 Tracor Lane, Austin, TX 78725.

Since the GLUAV is designed as an expendable system, the vehicle will terminate its flight near the target area. As a secondary goal of this analysis, it is desired to evaluate the possibility of using the GLUAV (after landing) as a stationary chemical weapons detection node. It is hypothesized that launching multiple GLAUVs in different directions could provide a sufficient number of chemical sensing nodes to relieve the burden of sending American personnel into potentially hostile territory to emplace current stand-alone chemical weapons detectors to protect U.S. troop concentrations. This functionality would depend on the battery life of the GLUAV and the ability to continue adequate air flow to the detector after the GLUAV comes to rest in what may be an undesirable orientation. Two assumptions will be assumed for this aspect of the analysis: 1) that the GLAUV will have sufficient power to run a chemical weapons detection system for some time after landing, and 2) that after landing, the chemical weapons detector's air passages will not be blocked.

The proposal for this project written by ARL personnel, which contains design requirements and guidance, is presented in appendix B. The proposal for this project was outlined in a meeting between the author and engineers at ARL in December 2002. While the attached document indicates that 1 mL/min is required to show functionality, that figure was based on information provided by other sources that have not shown functionality.

All design information is taken from the SolidWorks[3] assembly files for the GLUAV as well as ARL reports ARL-CR-466 (*2*) and ARL-CR-0515 (*3*). The GLUAV is designed to be launched from a conceptual 105-mm mortar or artillery weapons system and as such, the GLUAV is limited to a payload diameter of 1.75 inches and a total available payload length of 6 inches. ARL has estimated that the chemical weapons detection system should require no more than 3 inches of that total length. The total payload capacity is initially estimated to be 320 grams. As with any other aeronautical application, minimum weight is desired. Any concept that is created must have the potential of weighing less than the maximum payload in production form.

As the GLUAV is deployed from within a canister with its wings folded, any nozzles or other protrusions would be required to fit within a 0.1-inch gap between the folded wings. Figure 2 shows a side view of the GLUAV in its folded configuration as it would sit inside its deployment canister. Shown on the bottom of the GLUAV are the wings lying in parallel to the axis of the vehicle.

[3]SolidWorks Corporation, 300 Baker Avenue, Concord, MA 01742.

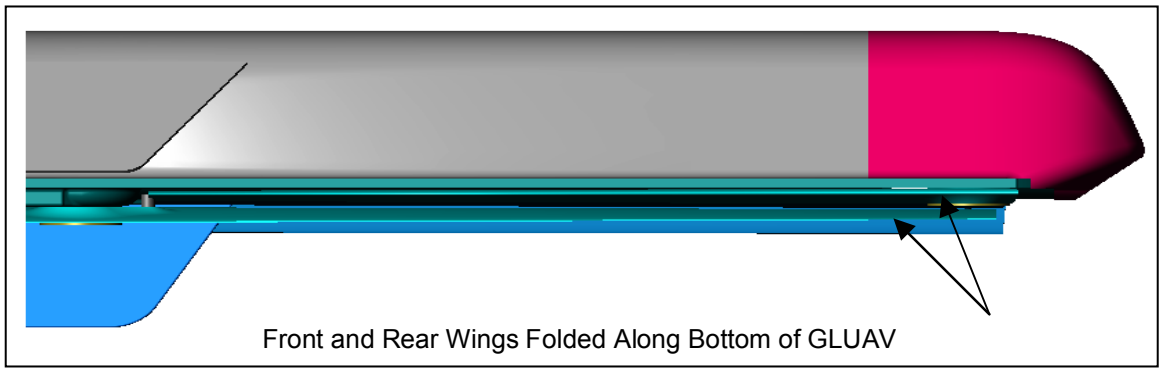

Figure 2. Side view of the GLUAV in folded configuration.

Figure 3 shows a view looking at the front of the GLUAV in the same launch configuration.

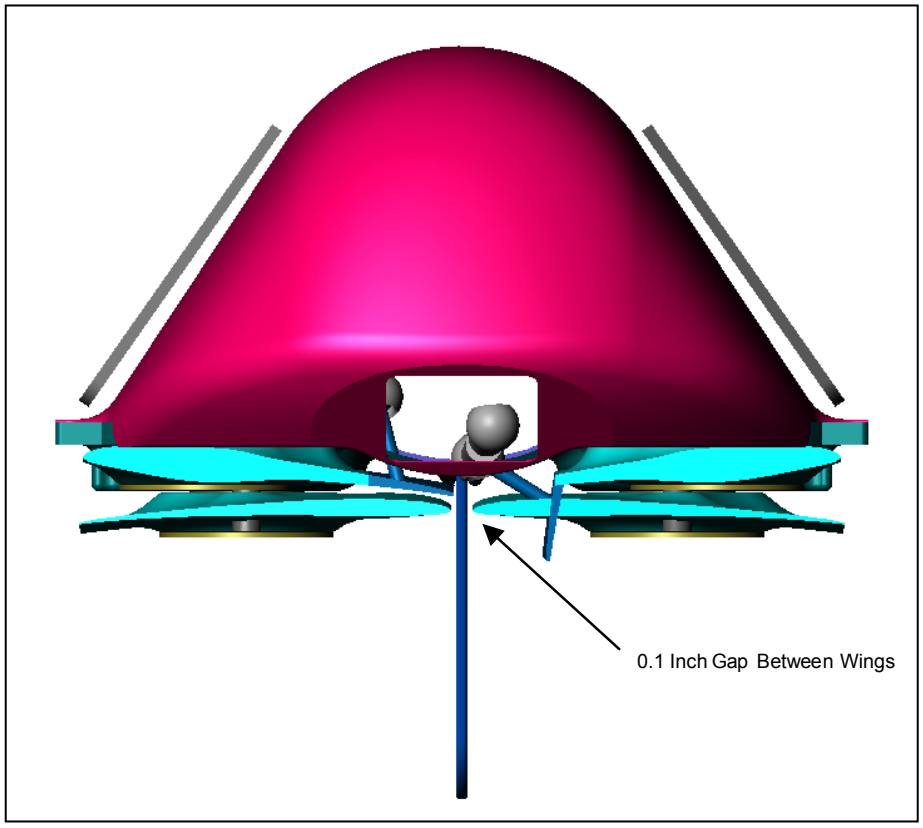

Figure 3. Front view of GLUAV in folded configuration.

Illustrated in figure 3 is the small 0.1-inch gap formed by the folded wings, which would require extensive design of any nozzles protruding from the GLUAV. ARL has also requested that any nozzles or protrusions from the GLUAV should be a maximum of 1 inch apart in the axial direction of the vehicle.

To determine the sustainability of air flow, it is essential to understand the conditions that the GLUAV will experience. In reference (*3*), the flight conditions of the GLUAV are provided. The velocity of the GLUAV ranges from a minimum of about 9 m/s to a maximum of about 20 m/s. The angle of attack (AOA) experienced throughout the flight profile varies from 0 degrees to a maximum of about 18 degrees. For the purpose of the study, the velocity range will be considered from 0 to 20 m/s and the AOA range from 0 to 20 degrees.

The GLUAV is designed for use on the tactical battlefield. In order to allow operations wherever U.S. Army soldiers are deployed, the chemical sensor must function in a wide range of conditions. ARL desired that for the purpose of this study, the examined altitude should range from sea level to 1000 feet (304.8 meters) above sea level. No specific temperature range was provided by ARL; however, it was decided to ensure operations between -20° C and 50° C.

Several different schemes were examined in the creation of a feasible design for this test. The initial concept relied on the use of the natural flow of air across the bottom surface of the GLUAV. It was thought that with proper design of the nozzles, it would be possible to create the needed air flow by managing the flow correctly. Because of the gap between the wings, two ideas were considered for nozzles. The first was a fixed nozzle that would "mushroom" out below the folded wings and be narrow enough at the given position to allow for the small wing gap. The second idea was to use an intake nozzle that would be spring loaded and pop out from the body of the GLUAV when the wings deployed. This would remove the flow restriction imposed by narrowing the nozzle to fit within the 0.1-inch dimension. Finally, an induced flow configuration was also considered in which a small blower would be placed inside the GLUAV to force air through an orifice and air passage.

2. Theory

To analyze the different ideas, the basic assumptions of the model were decided. The key decision for the model was whether to use a compressible or incompressible model. The incompressible flow model can be used if the fluid flow meets the following condition (*1*):

$$\mathrm{Ma} \leq 0.3 \tag{1}$$

in which Ma is the Mach number given by the following equation (*1*):

$$\frac{V^2}{a^2} = \mathrm{Ma}^2 \tag{2}$$

in which V is the velocity and a is the speed of sound in the given fluid. The speed of sound in a fluid is calculated according to the relationship (*1*)

$$a \approx (k\mathrm{RT})^{1/2} \tag{3}$$

in which T is the fluid temperature, R is the gas constant, and k is given as c_p/c_v.

After one selects the model to use, it is possible to determine the boundary layer effects according to the following sequence. To analyze the flow of the fluid over the body of the GLUAV, the Reynolds number is found by the equation (*1*)

$$\mathrm{Re} = \frac{\rho V L}{\mu} \tag{4}$$

in which ρ is the fluid density, V is the fluid velocity, L is the given length, and μ is the coefficient of viscosity. Making the assumption that the resulting fluid will be laminar, given by $\mathrm{Re} < 10^6$, the thickness of the boundary layer is given as (*1*)

$$\frac{\delta}{x} \approx \frac{5.0}{\mathrm{Re}^{1/2}} \tag{5}$$

in which δ is the boundary layer thickness and x is the position of the point in question. However, this equation only holds for fluid flow parallel to the surface of the body. To verify the results of these equations and to study the effects of varying AOAs, finite element analysis (FEA) software is used to simulate the flight conditions that the GLUAV would encounter during its normal flight profile.

3. Theoretical Analysis

To determine whether an incompressible model is acceptable, the Mach number in air must be determined. Given the need to use the GLUAV in typical battlefield conditions, it has been decided that calculations must be made with the assumption of a minimum operating temperature of -20° C and a maximum temperature of 50° C. Although this range does not accommodate every possible condition, it will cover the vast majority of potential operating situations. Given this temperature range, the speed of sound in air is calculated according to equation 3 and is found to vary from 320.19 m/s to 360.34 m/s. Substituting these values into equation 2 along with the maximum velocity of the vehicle of 20 m/s, it is found that the Mach number ranges from 0.0555 to 0.0625. This range certainly falls well below the threshold for the incompressible fluid model given in equation 1. With this information, the rest of the analysis and work performed will be conducted with air treated as an incompressible fluid.

With equations 4 and 5, the maximum boundary layer thickness can be found. The Reynolds number must first be determined with the use of GLUAV's altitude requirements. Since the operating parameters of the GLUAV require functionality between 0 and 1000 feet, the density

of the atmosphere is required at those points. For simplicity, the maximum altitude will be assumed to be 500 meters. Therefore, the minimum and maximum for the altitude will be sea level and 500 meters—a wider range than required. Density of the standard atmosphere at sea level and at 500 m is 1.2255 kg/m^3 and 1.1677 kg/m^3, respectively (*1*). Since the maximum boundary layer will occur at the rear of the body of the GLUAV, the characteristic length used is the entire length of the vehicle or 25.4 cm. The coefficient of viscosity of air, μ, is 1.8 x 10^{-5} kg/(m•s) (*1*). Equation 5 indicates that the boundary layer will be maximized by a low Reynolds number. Therefore, the minimum case for the Reynolds number will be found when the velocity is at a minimum and the density is at its minimum. With the density at 500 meters and the minimum velocity of 8 m/s, Re = 131820.35. With the rear of the vehicle as the position for equation 5, the maximum boundary layer is found to be approximately 3.50 x 10^{-3} meters. The maximum Reynolds number is found with equation 4 to be 345863.3, which validates the assumption that flow is laminar and that the correct equations were chosen to model the air flow.

To verify the basic analysis illustrated here, the FEA program ADINA[4] (automatic dynamic incremental nonlinear analysis) was used to calculate the velocity field across the body of the GLUAV. While FEA analysis is very useful to calculate exact solutions, attempts were made to keep the model as simple as possible and only use the solutions as predictions of trends. Figure 4 shows the geometry created for the analysis surrounded by the surfaces that were meshed and analyzed.

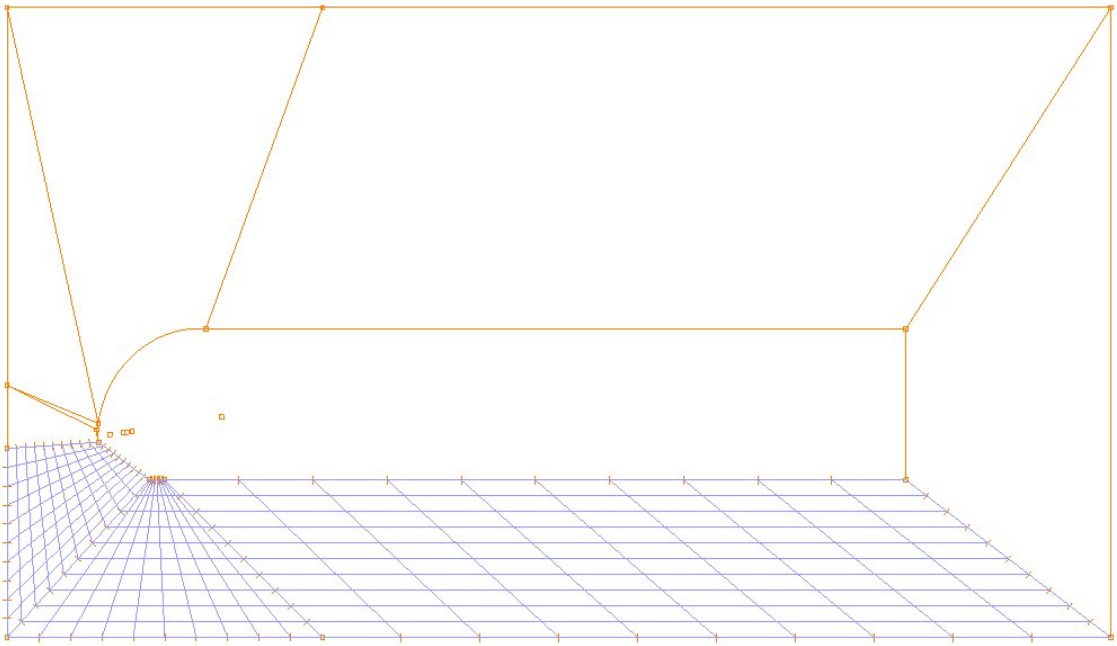

Figure 4. Outline of GLUAV geometry for ADINA analysis.

[4] ADINA R&D, 71 Elton Avenue, Watertown, MA 02472.

The bullet-shaped area in the center represents the side profile of the GLUAV as if a cross-sectional view were taken along the axis of vehicle. It is understood that this is a two-dimensional analysis of a three-dimensional problem, and the answers obtained by ADINA will not be exact for the three-dimensional case. However, the ADINA analysis will illustrate trends that will occur in the real case and should mirror the answers obtained through equations 4 and 5. The geometry was taken from the SolidWorks assembly files of the current design. Although the total lengths are all exact, the curve on the nose of the GLUAV is not exact because of translation difficulties from the spline curve that defines the nose profile to the ADINA model. Although the shape of the nose may not be precise, it is believed that any slight differences will not have a significant effect on the analysis of air flow across the bottom surface toward the rear of the airframe. Four different analyses were attempted with the minimum and maximum velocities, coupled with the minimum and maximum angles of attack. Because of computer hardware limitations, the mesh size could not be refined as much as desired; however, the analysis conducted did help us understand the air flow conditions through the estimated flight range of the GLUAV.

In figures 5 through 10, the length of the vector arrows indicates the magnitude of the air velocity. This magnitude is also represented by the gray scale coloring present. Some figures have different color coding, depending on what was chosen to make the figure most readable.

Figure 5 shows the first analysis run in which there is an 8-m/s ambient flow past the GLUAV at 0 AOA. The vertical dimension of the meshed area is 0.05 meter; each element in the FEA mesh is then 5 mm. ADINA therefore predicts that the boundary layer will actually be closer to 8 or 9 mm as opposed to the 3.5 mm predicted by equation 5.

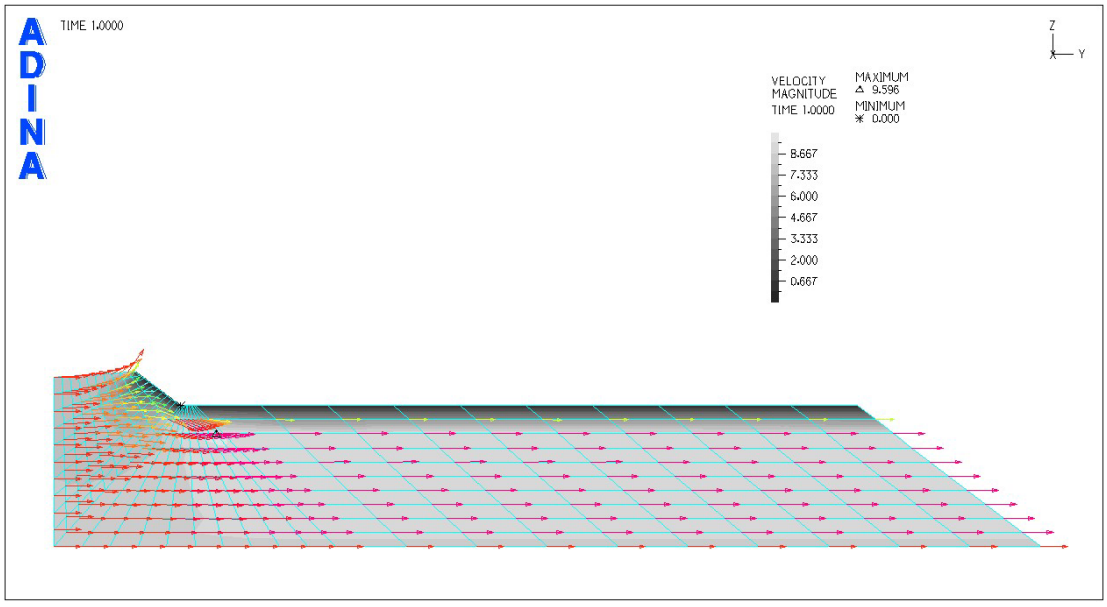

Figure 5. Air flow across bottom surface of GLUAV at 8 m/s, 0 AOA.

A similar figure is seen for ambient air flow of 20 m/s at a 0-degree AOA. As predicted by equation 5, the boundary layer is thinner than at lower speeds.

Figure 6 shows the velocity field of the air passing by the GLUAV at an air speed of 8 m/s and a 20-degree AOA. It is shown that as the AOA increases, the boundary layer decreases in size and a sizeable portion of the air near the vehicle is actually traveling faster than the ambient air flow.

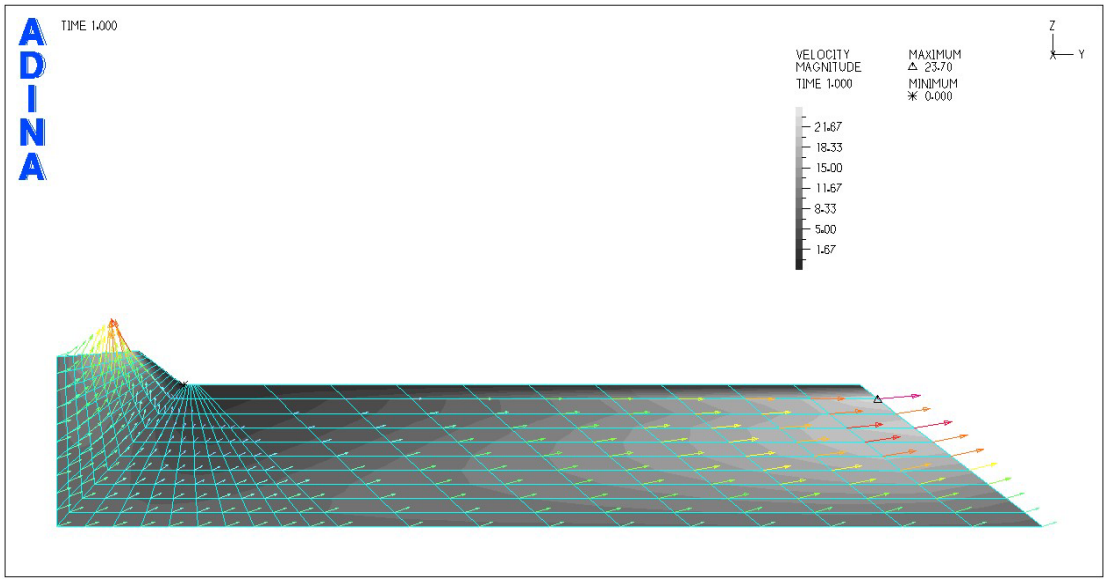

Figure 6. Air flow across bottom surface of GLUAV at 8 m/s, 20 AOA.

Figure 7 shows a similar velocity field for the vehicle as it travels at a 20-degree AOA at 20 m/s. It is noted that the velocity field is almost identical in shape as for the 8-m/s flow.

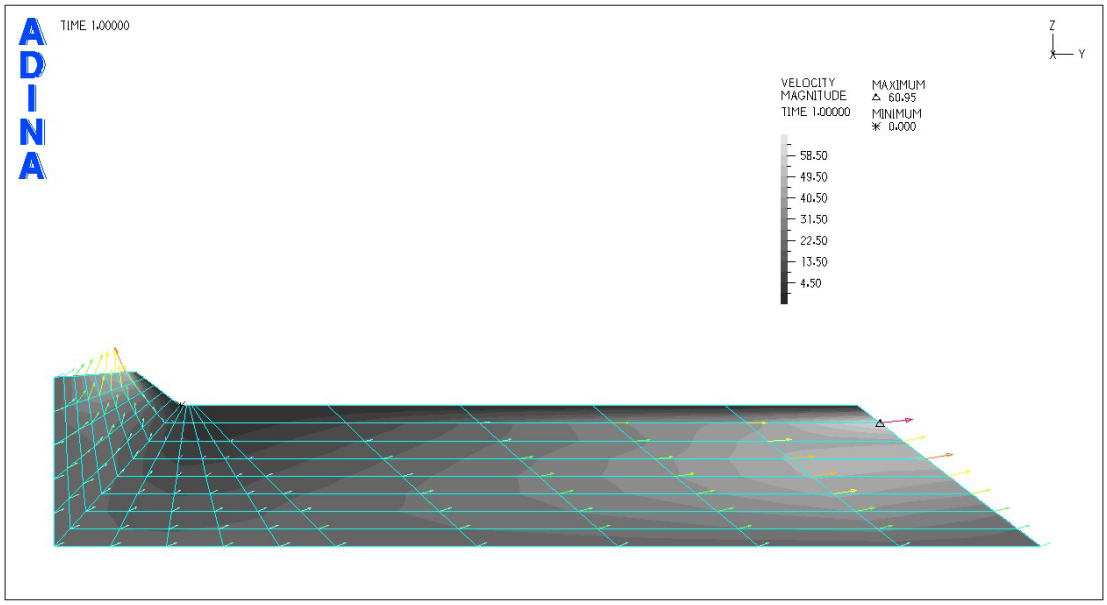

Figure 7. Air flow across bottom surface of GLUAV at 20 m/s, 20 AOA.

Given that such different conditions exist, depending on the flight conditions, it was decided that it would be difficult to determine exactly the shape of a nozzle to capture the needed air flow for all conditions. In addition, any nozzle that was designed would require two 90-degree bends in addition to a dramatic constriction needed to fit between the wings of the folded GLUAV. This constriction and bends would increase the back pressure and make it more difficult to design a nozzle capable of providing the needed air flow. For these reasons, it was decided to investigate the possibility of using forced induction to acquire the needed air flow.

To analyze the flow of air through a possible forced induction system, another simulation was run with a simulated inlet channel. This geometry and analysis used in ADINA in no way accounts for the blower that would be installed in the GLUAV. Instead, it establishes how the ambient air flow and AOA would impact the natural flow of air through the induction passageway. Figures 8 and 9 show the air flow across the GLUAV with a mock passageway as the vehicle travels at 20 and 8 m/s, respectively, at an AOA of 20 degrees.

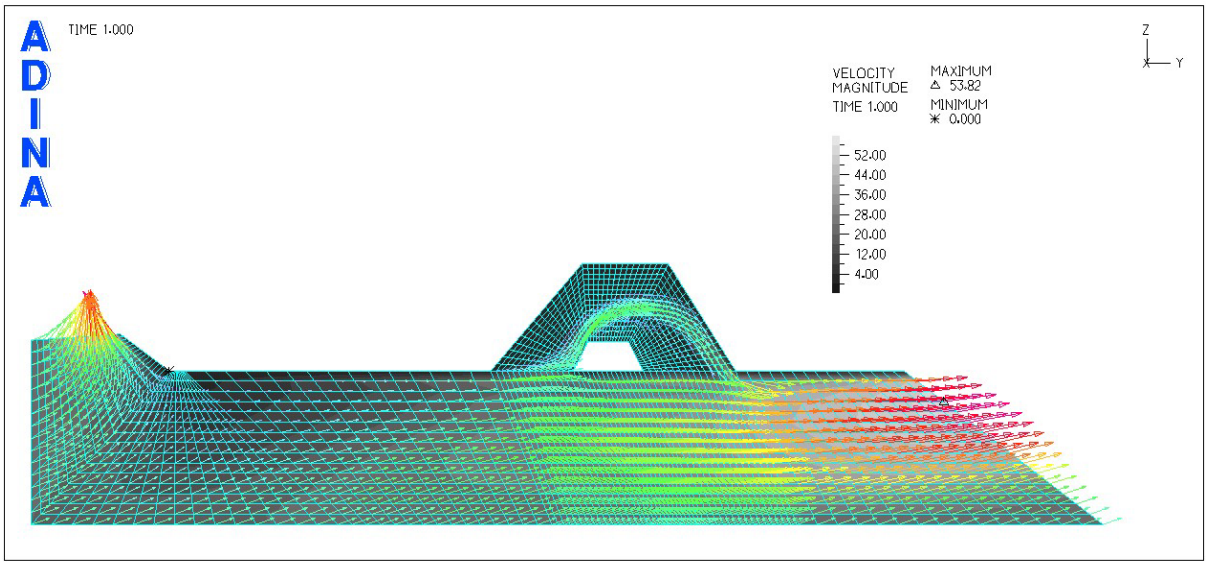

Figure 8. Air flow through inlet at 20 m/s, 20 AOA.

This analysis shows that the natural flow of air does indeed impact the sensing area of the GLUAV while it travels at high AOAs. The effect seen is to increase the total flow through the passageway, causing higher air flow than at lower AOAs. Although this effect is noted for both minimum and maximum velocities, it happens to a much lesser extent at 8 m/s. This effect is not seen at an AOA of 0. In figure 10, we see the velocity plot of air flow as the GLUAV travels at 20 m/s with a 0 AOA.

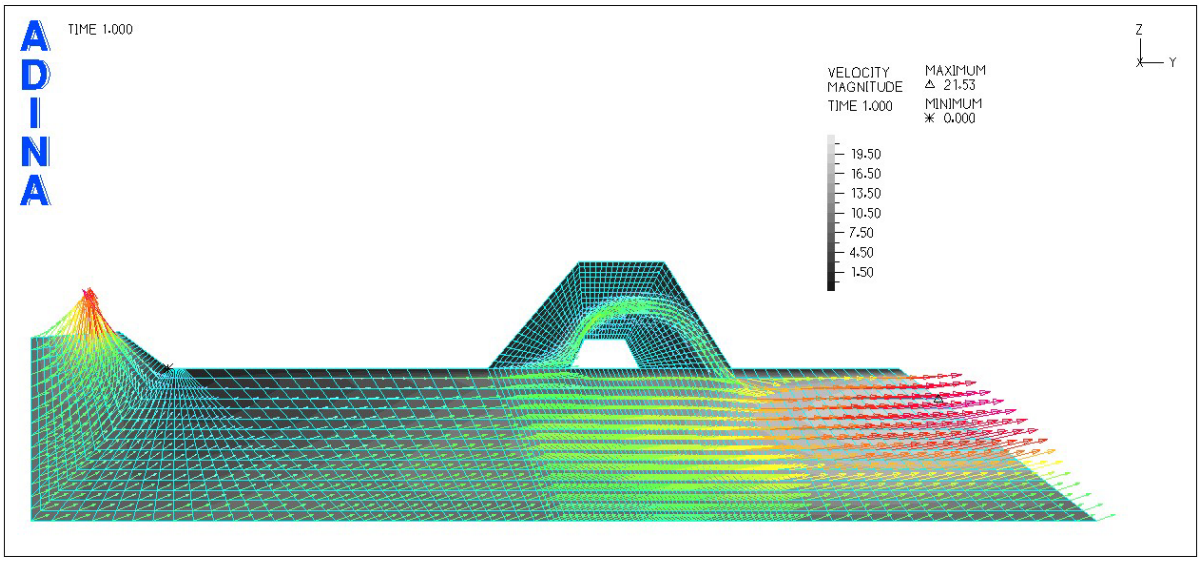

Figure 9. Air flow through inlet at 8 m/s, 20 AOA.

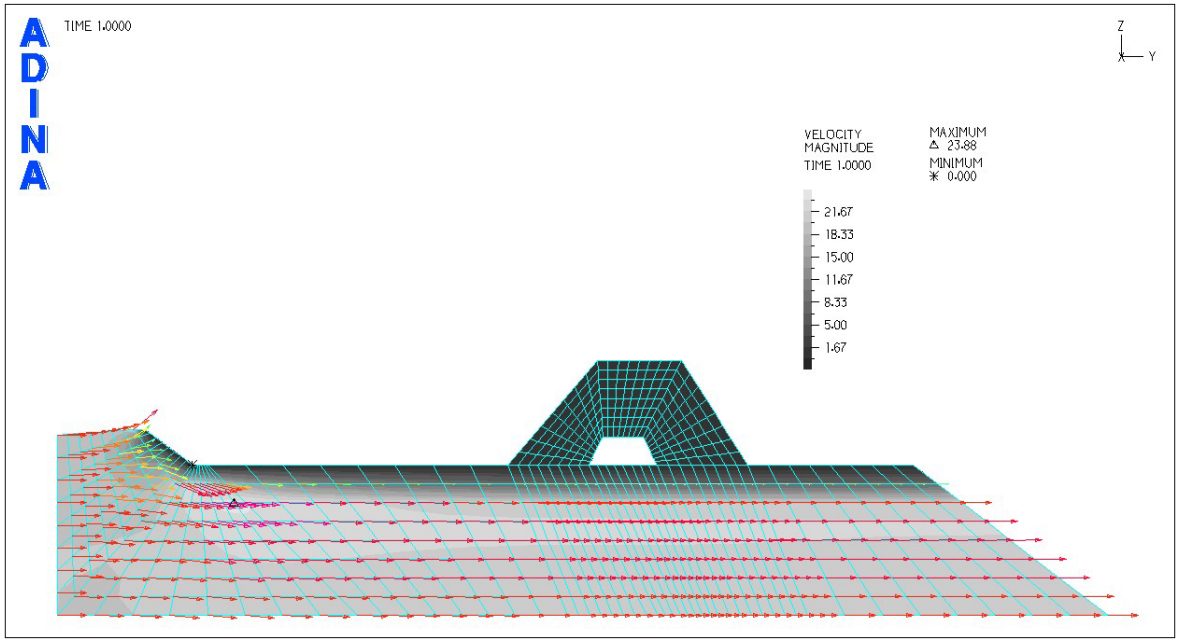

Figure 10. Air flow through inlet at 20 m/s, 0 AOA.

When the GLUAV is traveling at 0 AOA, there is negligible air flow through the passageway. This would indicate that if a blower were installed, the flow rate through the blower would be similar to the flow rate in a zero velocity condition.

By changing to forced induction, the need for designing nozzles is discarded and the needed flow of air is much easier to achieve. With a blower system, there are also other advantages. For example, only an intake and exhaust orifice would be needed. This would simplify production since the only changes in the airframe would be the drilling of two holes in the bottom surface as opposed to making either fixed nozzles or a spring-loaded system. Finally, a forced air induction system would assure functionality of the chemical sensor after the GLUAV has landed. Based on these preliminary conclusions, it was decided to further pursue the induced flow concept through experimentation.

4. Materials and Apparatus

Based on the results of the analysis, it was decided that forced induction would alleviate not only the analytical difficulties but also guarantee sufficient air flow if designed to be of sufficient size. With simple holes instead of nozzles as inlet and exhaust orifices, the size constraint of 0.10 inch imposed by the folded wings no longer has an impact on the design, and the size of the holes can be enlarged. A conceptual blower system was then designed to serve as a proof of concept. Any chemical system that would be designed would be required to fit into a configuration similar to that illustrated. However, since this is not intended to be a production level design, dimensions could change dramatically, depending on the results of testing. The design, shown in figure 11, consists of two plastic pieces that served as the air conduits and structure, a simple direct current (DC) motor, coupling shaft, and fan. The concept would mount in the GLUAV as shown in figure 12.

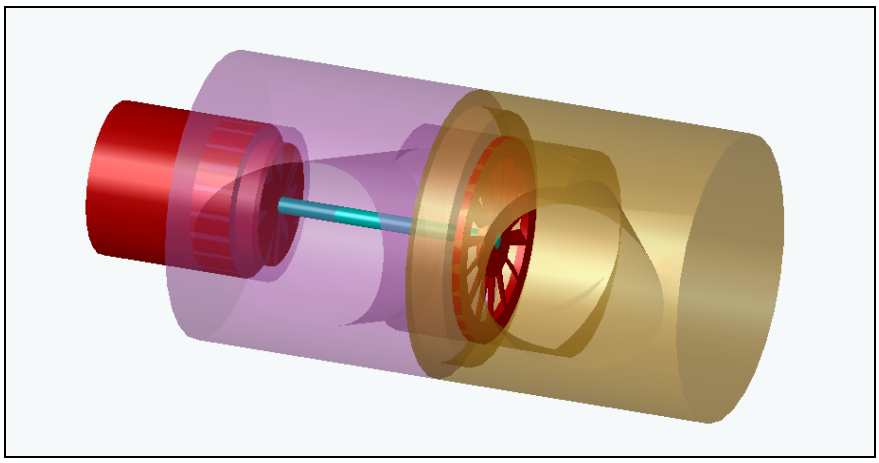

Figure 11. Concept design of blower assembly.

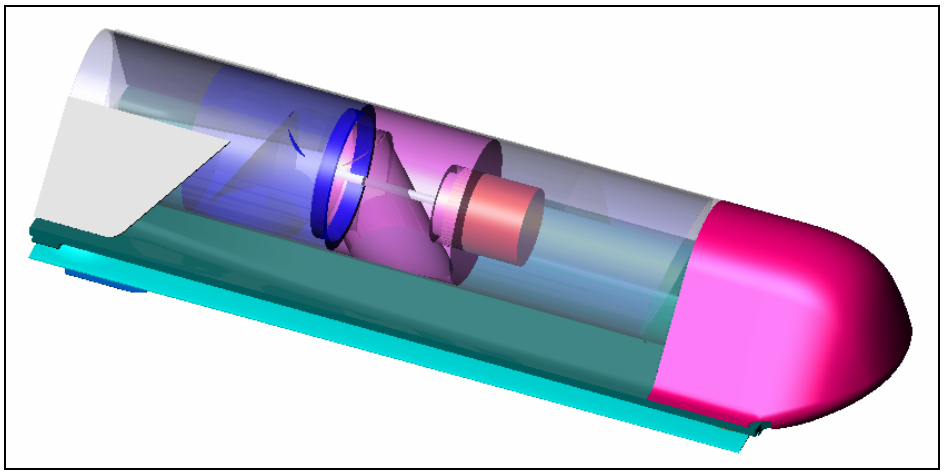

Figure 12. View of concept assembly installed in payload compartment of GLUAV.

In order to prove the functionality of such a system, a prototype was built. There was no attempt to create a production-ready prototype since any such system would need to be designed for the high-g loading experienced by the GLUAV. The intention was to create a prototype that could be evaluated to show that the needed air flow could be achieved during the GLAUV flight conditions. As such, this prototype is viewed as a proof-of-concept item.

In order to create a prototype, parts were designed on the basis of the concept shown in figure 12. Of the parts illustrated in the concept, only the housing needed to be designed and manufactured. The two parts composing the housing are shown in their corresponding drawings in figures 13 and 14.

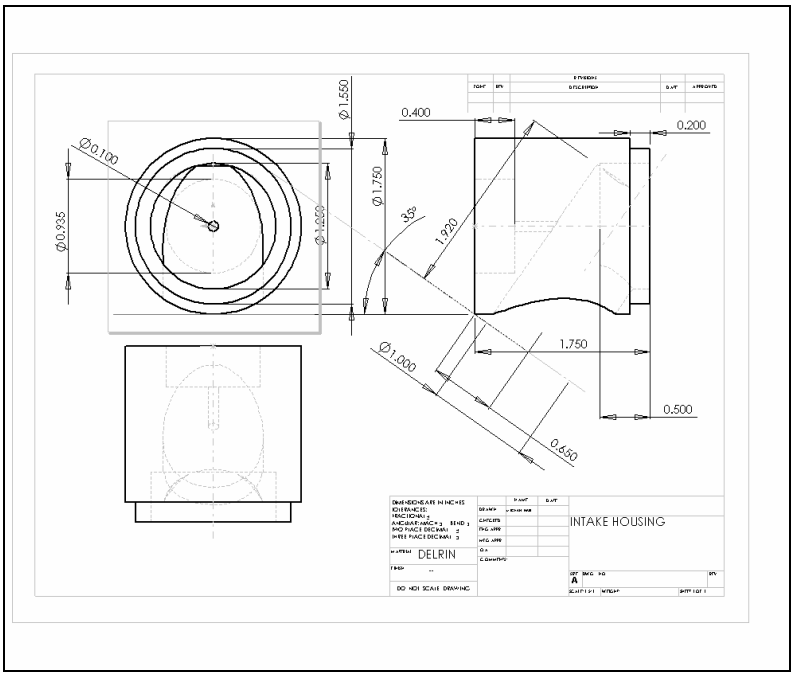

Figure 13. Drawing of the intake housing for prototype.

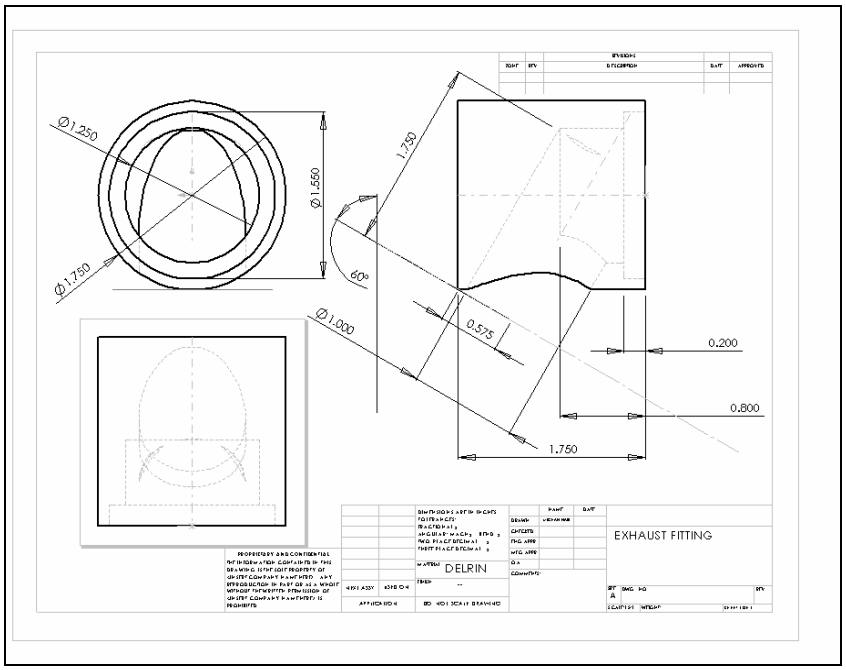

Figure 14. Drawing of the exhaust housing for prototype.

Both pieces were made from 2-inch diameter Delrin[5] stock. The stock was cut to shape with CNC mills and hand lathes at the Massachusetts Institute of Technology (MIT) Pappalardo Laboratory. A small DC motor (catalogue number 273-0223) was purchased at Radio Shack[6] for use in the device. The motor has a maximum no-load speed of 11,600 rpm and a stall torque of 53.0 G-cm at 3.0 volts nominal. The data sheet for the motor is presented in appendix C. A fan was taken from a small central processing unit cooler in the laboratory. The fan has a large central housing where the previous motor was mounted. The fan had a small stub protruding from the back side of the hub, which was connected to the DC motor via a coupling shaft made from 1/8-inch welding rod.

In order to facilitate testing, the device was mounted on a Plexiglas[7] base plate via 3-inch-long machine screws with holes drilled into the side of the device. To record the air velocity, a hot-wire anemometer was used. To facilitate accurate measurements, a small stand was made for the anemometer with Plexiglas. To ensure repeatability of measurements, a series of holes parallel to the axis of the device was drilled in the base plate 0.175 inch apart, which corresponded to a pin protruding from the base of the anemometer stand.

After fabrication and assembly of the pieces, the assembled device appears in figure 15 on a mounting plate and stand.

[5]Delrin® is a registered trademark of E.I. du Pont de Nemours and Company.

[6]Radio Shack® is a registered trademark of Tandy Corporation.

[7]Plexiglas® is a registered trademark of Röhm.

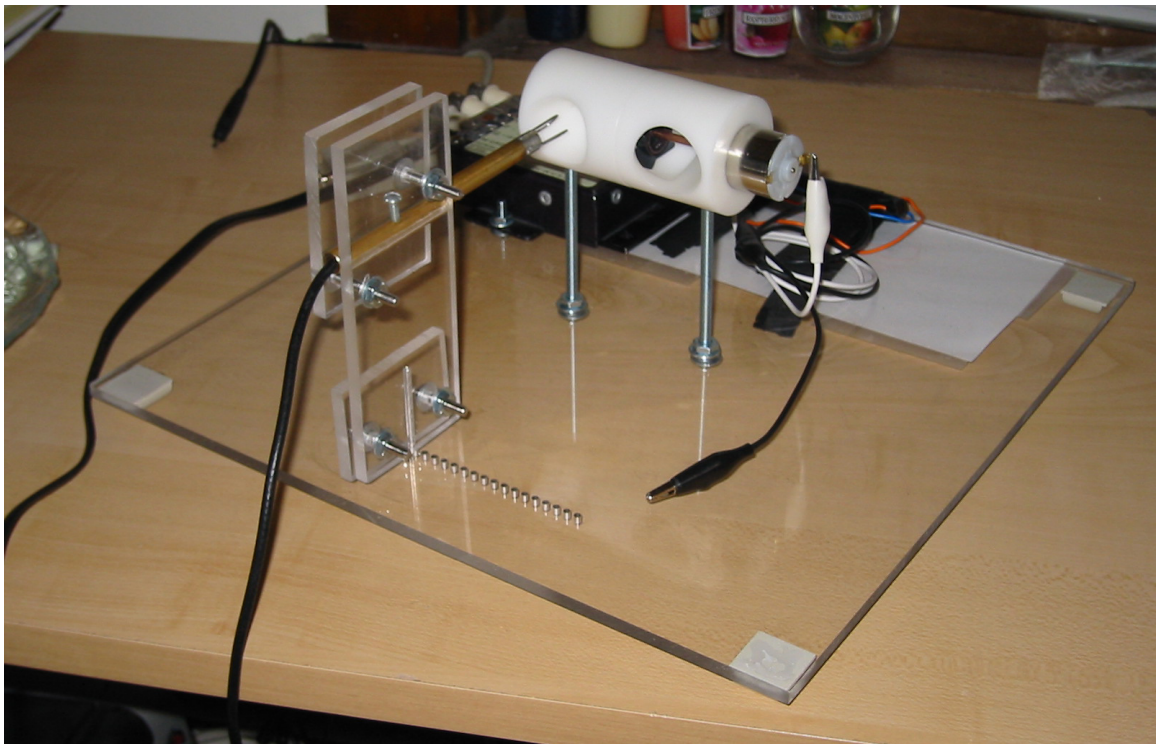

Figure 15. Assembled prototype on test stand with anemometer holder.

5. Experimental Procedures

To perform the experimentation, a simple setup and procedure was used. A hot-wire anemometer and associated control box was borrowed from the Undergraduate Measurement and Instrumentation Laboratory (UMIL) at MIT for the purpose of the experiment. The anemometer was calibrated with a manometer according to directions listed in appendix D, also provided by the UMIL. Note that the input voltage for tests at 0 and 3.5 m/s air flow was 11.9 volts, and the input voltage for the rest of the trials was 12.2 volts. The resulting equation relating fluid flow to velocity was entered into an Excel[8] spreadsheet. The anemometer control box was connected to a simple digital multimeter to record the voltage signal. The motor on the blower assembly was powered by two AA batteries, 2.98 volts, wired with "alligator" clips to the leads on the motor. The voltage on the batteries was monitored during testing to ensure that it was constant throughout testing.

With the test stand previously shown, experiments were run at wind speeds of 0, 3.5, 10, 15, and 20 m/s. For the 3.5-m/s speed, a standard room fan was used to provide the air flow. For higher speeds, normal fans were not sufficient and the device was mounted on the roof of an

[8]Excel™ is a trademark of Microsoft Corporation.

automobile. For each wind speed, the flow velocity through the orifice was measured at AOAs of 0, 5, 10, 15, and 20 degrees. To measure the air flow, the anemometer wire was oriented in the vertical direction, while the movement of the anemometer to sample the air flow was in the horizontal direction. For each data point, the voltage of the anemometer was recorded and entered into the Excel spreadsheet. Figure 16 shows a top view sketch of the setup showing the orientation and configuration of the device and anemometer.

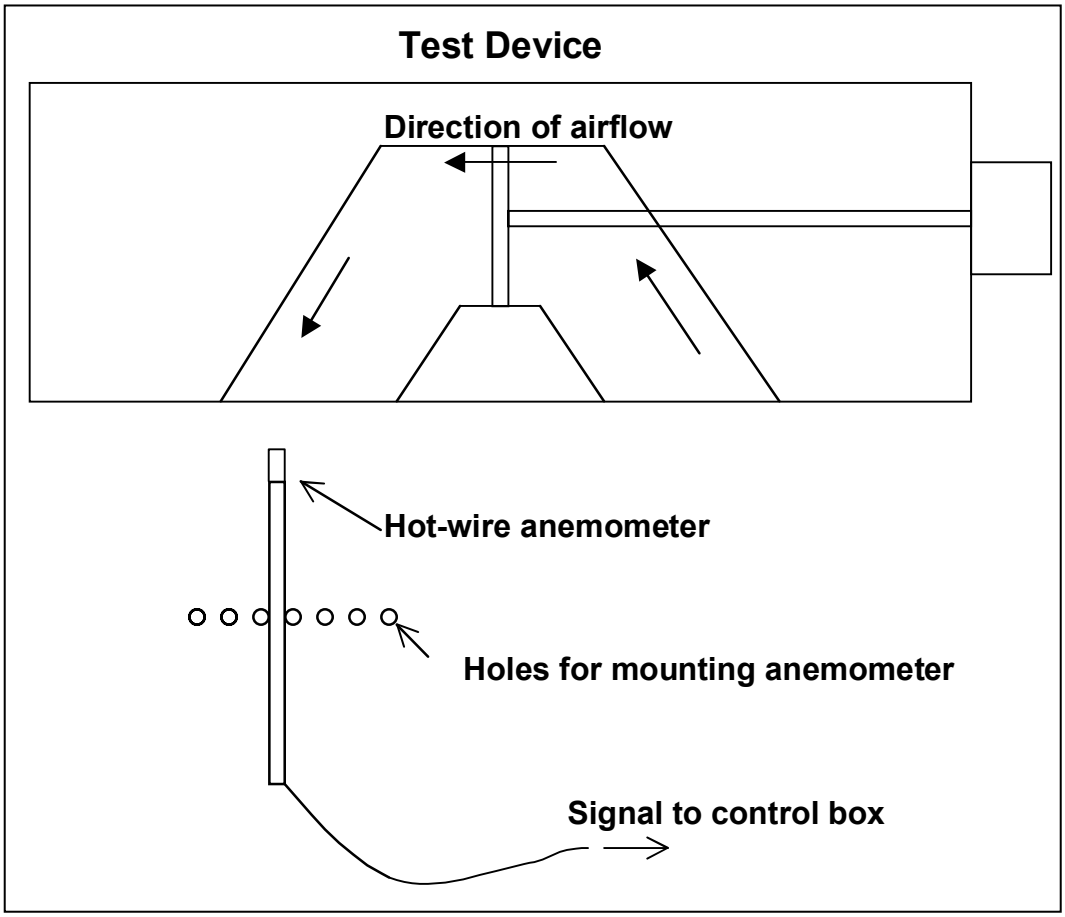

Figure 16. Schematic of experimental setup.

To calculate the volumetric flow, the velocity of the air is integrated over the area of the orifice. In order to simplify the integration, two assumptions are made: 1) that the air flow is steady state and does not change along the length of the passageway, and 2) that air flow is constant along the vertical axis. These assumptions allow easy calculation of the volumetric flow rate. To determine the volumetric flow rate, the data points are translated to such a position as if the orientation of the anemometer mounting holes were perpendicular to the axis of the exhaust opening. To translate the data points, the position of each of the holes was multiplied by the cosine of 30 degrees, which is the angle formed by the air passageway and the line of holes. This new line of data points is perpendicular to the axis of the hole so the opening is then a simple circle as opposed to the more complicated ellipse. To determine the flow rate, an

equation representing the flow must be determined. This expression is found through the use of Excel's curve fit feature. Because of the unusual shape of the data, a sixth order polynomial was selected to model the data. This equation was then multiplied by the equation of the circle, given by $r^2 = x^2 + y^2$, in which r^2 is 1.27 cm. This expression is then integrated across the opening of the circle and gives the volumetric flow rate.

6. Results

The results of the experiment were very well matched to the model's predicted behavior. Figure 17 shows the air flow velocity when the ambient air velocity is zero, along with the regression curve. The X-axis shown for all graphs has been normalized so that the middle of the air passageway is zero. The device in these figures is oriented 180 degrees from the depictions in ADINA so that position -1.15 cm is toward the rear of the device and 1.15 cm is the front.

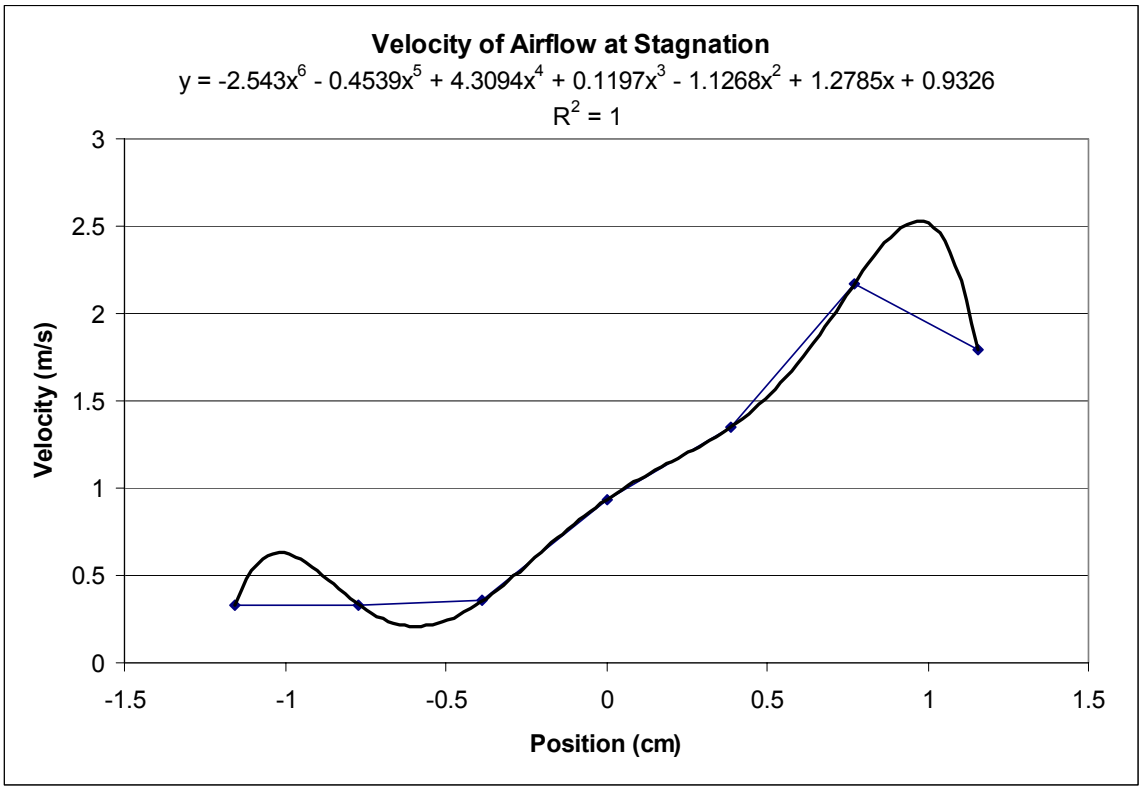

Figure 17. Velocity measurements at 0 m/s air flow with regression curve shown.

The regression curve given by Excel is shown on the top of the figure with the accompanying R value. The limits of integration chosen are from -0.01265 to 0.01265m. Although these numbers actually correspond to a smaller orifice than exists, it allowed for the thin layer of stagnant air immediately near the surface of the air passageway. The equation for the circle

representing the orifice area is given as $x^2 + y^2 = 0.00016129$. The flow rate is then calculated to be 2.362×10^{-4} m^3/s. This is then converted to liters per minute and found to be 14.17 L/min. The results for the 3.5-m/s ambient flow are given in figure 18.

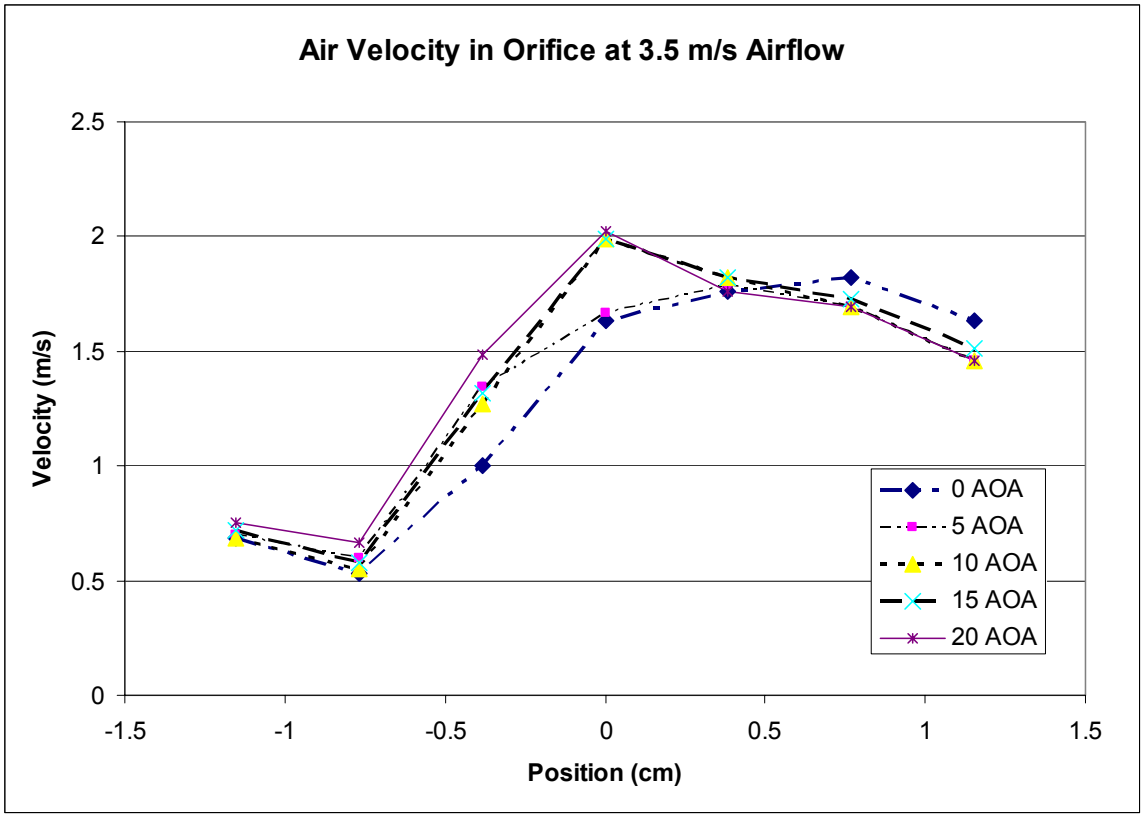

Figure 18. Velocity measurements at 3.5 m/s air flow.

To determine the volumetric flow rate at 3.5 m/s, only one of the data curves, 5-degree AOA, was selected since all the data curves are observed to be similar. As before, a sixth order polynomial was used to model the curve, and the curve was then integrated with the same parameters as given earlier. The data and the polynomial expression are shown in figure 19.

With the same process for the 5-degree AOA measurement with an ambient flow of 3.5 m/s, the flow rate is calculated to be 25.28 L/min.

Although the data points for higher velocities were taken, it was noted that the air flow velocities were similar to those measured at 3.5 m/s. For this reason, fewer data points were recorded for the 10-, 15-, and 20-m/s trials. Additionally, linear regression and exact calculation of the flow rate were not performed. The recorded velocities for these trials are shown in figures 20 through 22.

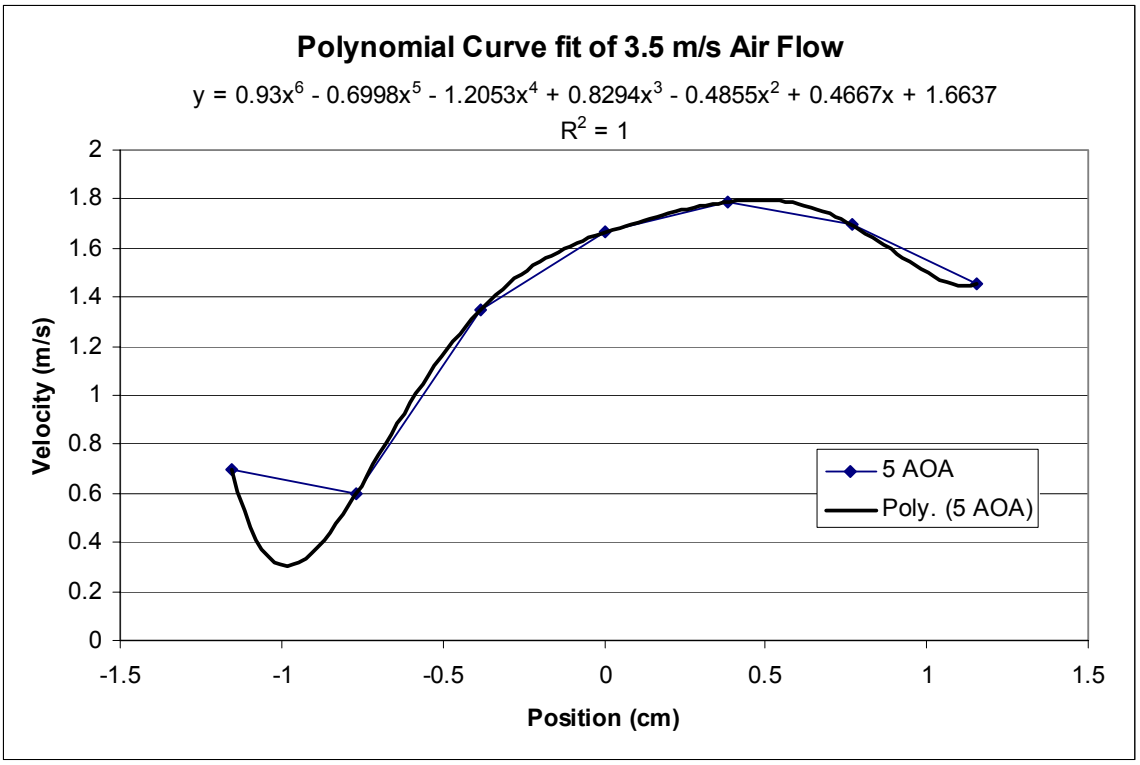

Figure 19. Regression curve fitted to 3.5 m/s, 5 AOA air flow measurements.

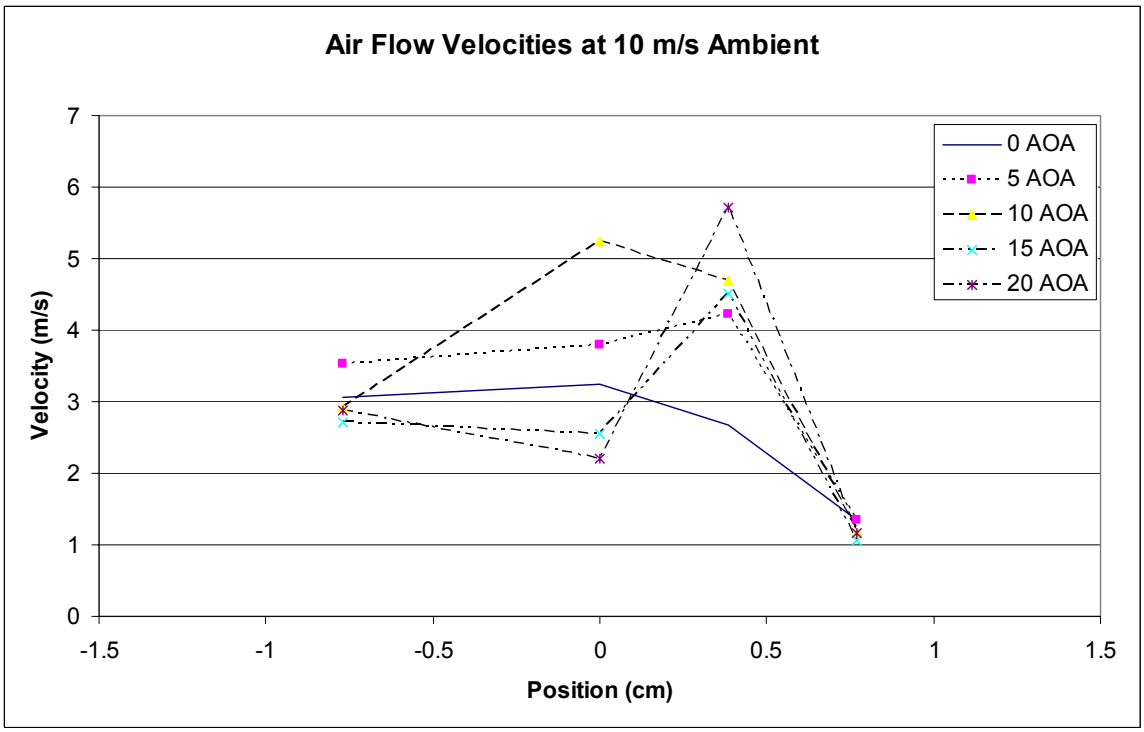

Figure 20. Velocity measurements at 10-m/s air flow.

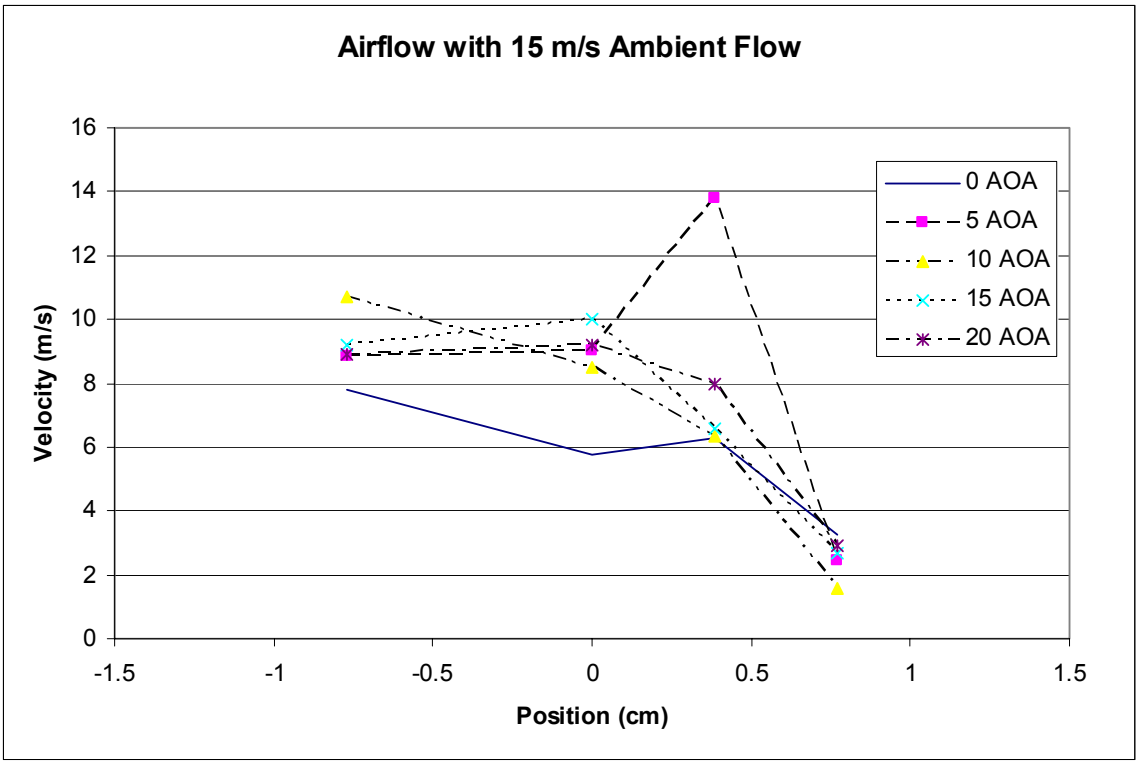

Figure 21. Velocity measurements at 15-m/s air flow.

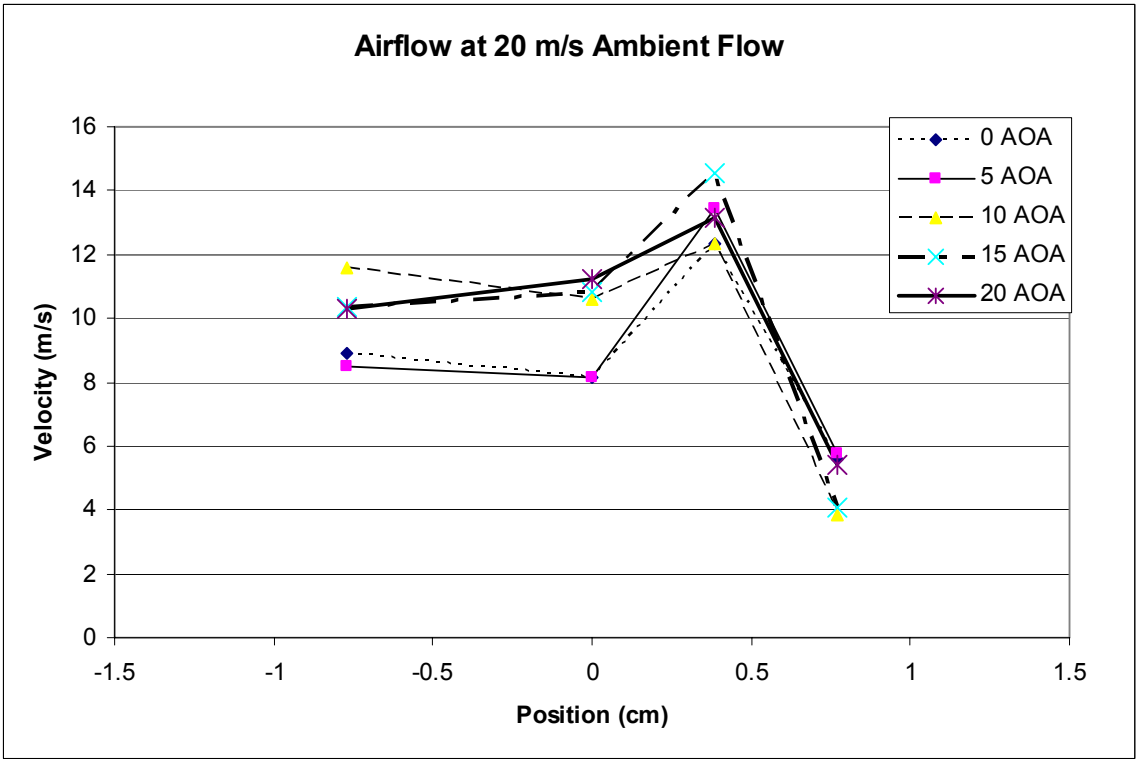

Figure 22. Velocity measurements at 20-m/s air flow.

7. Discussion

The experiment conducted proved that it is quite easy to obtain the needed air flow with induced flow. Even at stagnation flow, the simple blower device constructed here forces a volumetric flow rate ~10 times greater than what is required for chemical detector functionality. When the ambient air flow velocity was increased, the flow rate through the device also increased. Although it was not calculated explicitly for the higher velocities, it can be seen that the flow rate increases with ambient air velocity through the range measured. For the cases of 10-, 15-, and 20-m/s ambient flow, the measured orifice air velocity did not drop below 1.8 m/s. As shown by the figures, the recorded velocities for these three trials were noticeably higher as a whole than the lower speed trials, which indicated that the air flow through the device at these velocities is also significantly higher than needed. Since the intent of this experiment was to prove the sustainability of the needed air flow, calculation of the volumetric flow rate was not performed for the higher ambient air velocities since it can be seen from figures 21 through 23 that the volumetric flow rate will be sufficient. It can therefore be concluded that the air flow through the orifice at all conditions will easily surpass the required minimum air flow for chemical weapons detection.

As mentioned earlier, an automobile was used to achieve the needed velocities. It is likely that these velocities were not exact, since most speedometers are inaccurate by several percent. However, given that the device seems to produce a flow many times greater than needed, this difference is probably negligible. If it is desired to know the exact flow through the device, then more precise equipment would be needed to establish the ambient air flow.

It is also worth noting that the data seem to strongly support the model given by ADINA. The figures printed from ADINA show that with higher AOAs, air will begin to flow naturally through the passageway, augmenting the induced flow. Note that ADINA predicts that most of the flow will be pressed against the back wall of the exhaust orifice. This effect is seen in the changes of the curve from the lower velocity trials to the higher velocity trials. In the lower speed trials, the minimum speeds are recorded closest to the back wall of the exhaust, and the speed increases as the anemometer was moved toward the front of the device. This increase is not as noticeable and there is even a decrease as the probe is moved to the very front of the vehicle during the higher velocity trials. This effect indicates the accuracy of the ADINA model since it did predict trends that were later detected experimentally.

Although this demonstration showed that air flow is far beyond what is required, many changes could be made to improve the design. Several aspects of this proof-of-concept device lead to very significant losses in efficiency. First, the fan used has a large hub in the center. This reduces the fan efficiency since a smaller percentage of the passageway was actually being used to push air and the hub in the middle adds resistance to the flow of air. In addition, the fan could

be better sized for the orifice in which it sat. In the case of the device made, there was a sizeable gap between the diameter of the passageway and the fan blade. A smaller gap would also lead to more efficient flow. As can be seen in the drawings presented earlier, the housing that was machined had many sharp corners which led to interrupted air flow, also causing resistance to the air flow. Elimination of these corners and a more efficient shape could alleviate this flow impediment.

8. Conclusions and Recommendations

From the data acquired, it can be conclusively stated that a simple induced air flow system will easily achieve the volumetric flow rates needed to ensure operability of a chemical weapons detection system in ARL's GLUAV. This functionality has been predicted analytically, and experiments have proved this prediction.

For a production version of this system, numerous improvements could be made, and many were previously mentioned. One key change for production could be shrinking the entire package to make it smaller and lighter. Because the air flow in this demonstration device performed beyond the minimum air flow requirements without any effort being placed on air flow optimization, it is believed that a similar device, optimized for maximum flow rate, could be made significantly smaller. This smaller size would allow more usable payload for other items and more flexibility in the design of a chemical weapons detector for this system.

Based on the experiment, it appears that induced flow is indeed superior to the use of nozzles to duct the flow through the vehicle at the needed speed. With a design similar to that presented here, modifications of the GLUAV airframe are minimal and air flow is guaranteed and sustainable after landing.

In order to conduct a demonstration of this added capability for the GLUAV, the chemical sensor must demonstrate its ability to survive the extreme acceleration from launch, conform to weight, size and power constraints, and have a proven air induction system. Commercially available chemical sensors should be procured and then shock tested to determine their suitability for this application. Since most commercially available sensors are larger than the form factor required for the GLUAV program, a demonstration airframe should be built for this purpose. Through dimensional analysis, it will be possible to enlarge the demonstration airframe to allow for experimentation with the available sensors and still provide valid data for GLUAV use. Combined with computational fluid dynamics, the demonstration airframe would develop and demonstrate the feasibility of a functional intake system for use with a currently available chemical weapons detector. After functionality of the sensor is demonstrated, the investment can be made to miniaturize the chemical sensor to fit into the available space on the GLUAV if it is deemed worthwhile.

9. References

1. White, F.M. *Fluid Mechanics*, Boston: WCB McGraw-Hill, 1999, p. 24, 773.

2. Miralles, C.T. *Feasibility Study: Gun-Launched Unmanned Aerial Vehicle Concept*; ARL-CR-466; U.S. Army Research Laboratory: Aberdeen Proving Ground, MD, 2001.

3. Miralles, C.T. *Gun-Launched Unmanned Aerial Vehicle Flight Demonstration and Concept Validation*; ARL-CR-515; U.S. Army Research Laboratory: Aberdeen Proving Ground, MD, 2003.

INTENTIONALLY LEFT BLANK.

Appendix A. E-mail Correspondence Regarding Volumetric Flow Rates for Chemical Weapons Detectors

1. E-mail regarding Environics ChemPro 100.

From: Mrphillip@aol.com
Date: Mon, 27 Jan 2003 07:12:55 EST
Subject: ChemPro Info
To: nair@mit.edu
X-Mailer: AOL 8.0 for Windows US sub 230
X-Spam-Not-Checked: Messages over 100K not checked
X-Scanned-By: MIMEDefang 2.28 (www . roaringpenguin . com / mimedefang)

Michael,

Attached is some info on the ChemPro 100 you requested. The airflow for the system is 1 liter/min.
4-Page Brochure-ChemPro - Nov 25 2002.ppt

2. E-mails from SBCCOM regarding military chemical weapons detectors.

Here is some info on a specific type of military Chemical Sensor which has been incorporated into vehicles. If you have particular questions about this specific detector, please contact Mr. Roger Griffin at 410-436-2112.

-----Original Message-----
From: Griffin, Roger L SBCCOM
Sent: Wednesday, February 19, 2003 2:57 PM
To: Vigus, Richard A SBCCOM
Cc: Griffin, Roger L SBCCOM
Subject: RE: HLD Products and Services Web Page

Rich- I'll again caution you and Mr. Nair that restricting or assisting the airflow into the ACADA introduces numerous questions and cautions- the major one Dan brought up with the membrane. We have mounted M22s/M88s within vehicles and the primary rule is to keep the line short and straight (and heated if possible).

Please have Mr. Nair call me with questions. The spec data on the pump assembly follows. Note that the airflow thru the M22 is twice the figures listed. We have two pump assemblies per M88 (one for the G side and one for the H side).

3.1.2 Air draw and energy consumption. With 2.25 0.01 V DC applied to the pump connector, the air flow rate through each cylinder shall be greater than 350 ml/min when the inlet is restricted to produce a suction pressure of 5.86 kN/m2 2% (0.85 0.02 psi). The air flow rate through each cylinder shall be greater than 500 ml/min when the inlet is restricted to produce a suction pressure of less than 0.53

kN/m2 (0.08 psi). The current consumption of the pump motor under these conditions shall be no greater than 130 mA.

Roger

-----Original Message-----
From: Vigus, Richard A SBCCOM
Sent: Wednesday, February 19, 2003 9:46 AM
To: Griffin, Roger L SBCCOM
Subject: FW: HLD Products and Services Web Page

Roger---Do you know what the power rating for the air pump in the ACADA is? We got a question from this guy doing a thesis at ARL related to feasability of installing chem sensors in vehicles---and he's asking some questions about pressure drop, etc...do you have that info?
-----Original Message-----
From: Nowak, Daniel M SBCCOM
Sent: Wednesday, February 19, 2003 9:37 AM
To: Vigus, Richard A SBCCOM
Subject: RE: HLD Products and Services Web Page

Rich, suggest you contact Engineering (Klein) on the older point samplers and Roger Griffin for the M22. They should have the specs for the pumps.
DAN
-----Original Message-----
From: Vigus, Richard A SBCCOM
Sent: Wednesday, February 19, 2003 9:27 AM
To: Nowak, Daniel M SBCCOM
Subject: RE: HLD Products and Services Web Page

okay, so how about the power rating of the air pump? perhaps with that info this guy can figure it out.
-----Original Message-----
From: Nowak, Daniel M SBCCOM
Sent: Wednesday, February 19, 2003 9:20 AM
To: Vigus, Richard A SBCCOM
Subject: RE: HLD Products and Services Web Page

I don't know this one. Blowing air into the point sensors is not a good idea since some have membranes which could be ruptured.
DAN
-----Original Message-----
From: Vigus, Richard A SBCCOM
Sent: Wednesday, February 19, 2003 9:13 AM
To: Nowak, Daniel M SBCCOM
Subject: FW: HLD Products and Services Web Page

Dan---Can you help?

-----Original Message-----

From: Garcia, Patsy R SBCCOM
Sent: Wednesday, February 19, 2003 8:47 AM
To: Vigus, Richard A SBCCOM
Subject: FW: HLD Products and Services Web Page

Can you answer this one?

-----Original Message-----
From: michael nair [mailto:nair@MIT.EDU]
Sent: Friday, February 14, 2003 4:43 PM
To: Garcia, Patsy R SBCCOM
Subject: RE: HLD Products and Services Web Page

Thank you for your response. I had one more question, I was wondering if you have any information regarding the pressure loss across the sensing element. For example, if I was to blow air through the sensor, what kind of a head loss would I have from the flow restriction. If you have any information relating to this, I would appreciate any help that you would be able to offer,
Sincerely,
Michael Nair

At 10:40 AM 1/28/2003 -0500, you wrote:

Typical military point sensors for chemical agents operate in the 1.2 1.4 liters/minute range for flow rate.

-----Original Message-----
From: michael nair [mailto:nair@MIT.EDU]
Sent: Wednesday, January 22, 2003 1:06 PM
To: homeland.defense@sbccom.apgea.army.mil
Subject: HLD Products and Services Web Page

Dear Sirs:
I working on my thesis project with the US Army Research Lab in Aberdeen, Maryland. The focus of my thesis is the feasibility of installing a chemical weapons detector on a concept vehicle. I am in need of information regarding typical minimum flow rates for detectors. If you have any information regarding this topic I would appreciate any help that could be offered.
Sincerely,
Michael Nair

Michael L. Nair
617-504-1067
94 Spring Street, Apt. 1
Cambridge, MA 02141
Michael L. Nair
617-504-1067

94 Spring Street, Apt. 1
Cambridge, MA 02141

[] smime.p7s

Appendix B. Project Proposal From ARL, Received on January 3, 2003

Senior Design Research Project for Michael Nair, senior ME Student Massachusetts Institute of Technology (MIT)

Title: Conceptual Design, Engineering Modeling, and Experimental Validation of Air Sampling System for Chemical Sensor Insertion into the U.S. Army Research Laboratory's (ARL) Silent Operating Aerial Reconnaissance (SOAR) Program.

Figure A-1. SOAR vehicle in flight (glider version).

Major Focus of Project:

1. Conceptual design and engineering modeling of air sampling system within constraints specified by ARL

a. Use of SolidWorks to perform computer-aided design/engineering from models provided by ARL.

System Constraints: All components must fit within payload tube (fuselage, 1.75-inch diameter) of SOAR model as defined in SolidWorks files. Length of payload tube available for sensor not to exceed 3.0 inches. Ductwork associated with the intake/ exhaust manifolds should not exceed 0.1 inch in diameter and should be less than 1.0 inch apart. Extension and air capture/exhaust direction will be determined by student during the design process. Current estimates indicate that the air sampling system should be able to pass ambient air across the detector surface at a minimum flow rate of 1 ml/min. Student will conduct a survey of existing hand-held chemical sensors to confirm or modify this flow rate. The design of the air sampling system should also take into account the expected operating characteristics at an altitude of 0 to 1000 ft above sea level (ASL), taking into account the vehicle's expected flight performance (angle of attack (AoA), velocity, bank angle, etc.) as specified in the provided technical reports. Other sampling system characteristics such as mass, volume, power requirements, sensitivity, response time, etc. will be determined by the student.

b. Predict the performance of the conceptual design using either analytical or computational fluid dynamics methods. Predict the performance through SOAR operating altitudes (1000 ft - ground) and various AoA of min. = 0 to max. = 20 degrees and velocities (velocity of min. = 9 to max. = 20 m/s) at CL = 0.8-1.0 (Miralles, 2003) to determine the operating AoA range at the CL being analyzed.

Table A-1. Sample set of variables for part 1b.

Altitude	AoA	Max Flow Rate
1000 Ft	a = AoA range	Ra
500 Ft	a = AoA range	Ra
Ground = 0 Ft	a = g (TBD at ground)	Rg

2. Using commercial-off-the-shelf (COTS) items, integrate a surrogate sampling system into the SOAR for purposes of wind tunnel experiments.

3. Experimentation in wind tunnel to validate conceptual design and predictions

a. Design an experimental setup and test matrix to verify selected data points in part 1b. Assistance will be provided for the location of a wind tunnel facility if one is not available at MIT.
b. Use a flow meter as a surrogate chemical sensor to measure the flow rate into the SOAR. Student will perform research and purchase/borrow the correct flow meter within performance and size constraints using COTS. If a flow meter is not readily available that meets the size constraints mentioned, the student can consider placing the meter outside and behind the airframe, with the ductwork fixed (but extended) within the airframe as originally envisioned. The student can explain differences and limitations of this meter setup compared to the ideal meter-within-the-airframe case.
c. Data will be recorded and saved from the flow meter experiments.
d. Analyze data to verify the validity of calculations in part 1b. If experimental versus calculated data disagree, try to determine why the calculated data do not match.

4. Document and/or present results

Final report to include design methodology, description of calculations, experimental data and analysis, and mechanical details (SolidWorks model).

Appendix C. Specifications Sheet for DC Motor Used in Prototype

SR-3 Motor
(273-0223) Specifications Faxback Doc. # 19830

At 1.5 V (Nominal Voltage):
- Resistance.....0.25 Ohm
- No Load Speed.....5700 RPM
- No Load Current.....0.20 A

At Maximum Efficiency:
- Speed.....4100 RPM
- Current Rating.....0.55 A
- Torque.....9.4 G-cm
- Power Used.....0.39 W
- Efficiency..... 45%

- Stall Torque.....33.5 G-cm

At 3.0 V (Nominal Voltage):
- Resistance.....0.50 Ohm
- No Load Speed.....11,600 RPM
- No Load Current.....0.25 A

At Maximum Efficiency:
- Speed.....8300 RPM
- Current Rating.....0.99 A
- Torque.....15.0 G-cm
- Power Used.....1.29 W
- Efficiency.....52%

- Stall Torque.....53.0 G-cm

Specifications are typical; individual units might vary. Specifications are subject to change without notice.

(IR-02/29/96)

INTENTIONALLY LEFT BLANK.

Appendix D. Anemometer Calibration

(Taken from "Volumetric Fluid Flow Measurement, Fall, 2002" from MIT course 2.671, courtesy of Dr. Barbara Hughey)

3. Calibration of Hot Film Anemometer and Positioner

A hot film anemometer is a common instrument for measuring gas velocity. Its operation is described in appendix B, where it is shown that the relationship between its output voltage V_{out} and fluid velocity u_g is

$$V_{out}^2 = C + D\sqrt{u_g}$$

in which C and D are constants. The only practical way to determine C and D is by experiment. The Pitot probe (appendix A) allows a simple determination of velocity u_g from a pressure measurement. As discussed in appendix A, it relies on the Bernoulli relation, in which the only physical constants necessary are fluid densities and the gravitational acceleration. A Pitot tube may therefore be used as a velocity measuring standard, from which the hot film anemometer may be calibrated (i.e., the values of C and D in equation 1 determined).

3.1 Hot Film Anemometer Setup

CAUTION: THE HOT FILM SENSOR IS VERY FRAGILE. BE EXTREMELY CAREFUL WHEN/IF YOU HANDLE THE PROBE.

1. Record the serial number and any other information on the anemometer box in your lab notebook. The sensor is already installed in a stainless tube that slides in the brass holder mounted on the translation stage at the end of the pipe. The clips extending from the brass tube are there to protect the sensor wire.

2. The sensor wire should be oriented vertically and positioned to face the free jet nozzle, which is connected to the house compressed air supply.

3. Turn on the E3610A power supply labeled "15V for Anemometer". The digital multimeter labeled "Anemometer" should read about 3.7 V. Blow gently on the hot film sensor. You should see the voltage output increase in magnitude. The hot film anemometer is now ready to be calibrated (sect. 3.3).

3.3 Calibration of Hot Film Anemometer

Please read appendices A and B before proceeding.

1. The Pitot tube is mounted on the positioner with thumbscrews and washers and should also be facing the free jet nozzle. The Pitot tube must be oriented parallel to the direction of air flow out of the nozzle, and the hot film sensor wire must be perpendicular to the flow direction. Make sure that both probes are at the same height as the nozzle tip and at the same distance from the nozzle. The positioner will be turned by hand (using the black knob at left of the positioner) to alternately place each probe at the centerline of the air jet.

2. The flow is adjusted with the regulator valve on the wall. Open the 1/4 turn shutoff valve on the wall by rotating the yellow handle so that it points down. Start with the regulator turned counterclockwise until the pressure gauge reads approximately 0 psi.

3. Record the "no-flow" manometer deflection and the "no-flow" anemometer output (in volts) in your lab notebook. **Look carefully at the gradations on the manometer scale, to make sure you read them correctly.** *Is the no-flow anemometer output constant? This is a very sensitive instrument; what could be causing error in your no-flow reading?* If you detect a non-zero manometer deflection, you should subtract its value from your subsequent measurements in order to correct for the slight offset of the two manometer columns with no flow.

4. Increase the pressure by turning the regulator valve clockwise until it reads about 4 psi. *Is this gauge or absolute pressure?* Place the anemometer at the approximate centerline of the air nozzle and move the positioner back and forth to find to point of maximum anemometer output voltage. Record the anemometer output and positioner output voltage at this location in your lab notebook.

5. Now place the Pitot tube at the approximate centerline of the air nozzle and move the positioner back and forth to find to point of maximum manometer deflection. Record the manometer deflection and positioner output voltage at this location in your lab notebook.

6. Without moving the positioner, decrease the pressure to produce an air flow sufficient to produce a manometer deflection, h_w (defined in figure 7) of about 6 mm or less. Allow time for the flow to stabilize. Measure and record this manometer deflection. In your analysis (step 10), be sure to correct for the initial manometer reading at zero air flow (if it was not zero).

7. Using the positioner, move the anemometer probe to the jet centerline, resetting the positioner at the location found in step 4, as determined by the pot output voltage. Record this value of V_{out}, as well as the positioner output voltage at this location. You should notice that V_{out} fluctuates while you are moving the positioner, and displays larger voltages while in motion than while still. Why does this occur? Which is the correct reading?

8. Increase the flow until V_{out} is approximately 7 V. Repeat this measurement sequence (reading the hot film probe first this time, then the Pitot probe first in the next sequence) for at total of six air flows (including the no-flow point). Reset the positioner for each sensor at the locations found in steps 4 and 5, as determined by the pot output voltage. Do not exceed 100 mm deflection of the manometer (V_{out} less than 8.3 V). Record the manometer deflection and V_{out} for each flow rate.

9. Turn the regulator fully counter clockwise and close the air flow shutoff valve (yellow handle horizontal).

10. Convert the manometer reading h_w to velocity u_g using the Bernoulli relationship (equation 14 in appendix A). The manometer angle θ is 30°. Do not forget to include your zero flow point. Present the data as a plot of V_{out}^2 vs $\sqrt{u_g}$. The plot should be a straight line. Perform a linear regression (you can use the Trendline feature in Excel[9]) to determine the constants C and D that appear in equation 19 in appendix B. Print the plot (including the equation and the R_2 value) and include in your lab notebook.

[9]Excel™ is a trademark of Microsoft Corporation.

Appendices

A. Flow Velocity Measurements With a Pitot Probe and Manometer

The Pitot probe works on the Bernoulli principle, which states that in steady flow of an incompressible fluid (or compressible fluid at low Mach number), the change in kinetic energy per unit mass between any two positions equals the work done on the mass by pressure, P, and gravity forces. For a fluid with flow velocity u and density ρ_g: constant

$$\left(\frac{u_1^2}{2}+\frac{P}{\rho_g}+gh\right)=\text{constant}$$

in which g is the acceleration of gravity and h is the fluid height with respect to a reference point. For the probe arrangement shown in figure 7, where $h_2 = h_1$, we may express equation 7 as

$$\frac{u_1^2}{2}+\frac{P_1}{\rho_g}+gh_1=\frac{u_2^2}{2}+\frac{P_2}{\rho_g}+gh_1$$

The Bernoulli constant at an arbitrary point 1 is unaffected by the presence of the Pitot probe at point 2. With $u_2 = 0$ (stagnation point), equation 8 may be solved for u_1, which equals the flow velocity u_g:

$$u_1 \equiv u_g = \sqrt{\frac{2}{\rho g}}\left(P_2 - P_1\right)$$

The pressure difference ($P_2 - P_1$) can be measured in a number of ways; one method is to use a manometer. The manometer is simple but has limited sensitivity, range, and frequency response. For this case where the fluid is air, P_0 (defined in figure 7) and P_1 are related as

$$P_0 = P_1 + \rho_g g h_1$$

For the "reclining" manometer (figure 7), with θ measured from the horizontal plane, as indicated in figure 7, pressures P_3 and P_2 are related as

$$P_3 = P_2 + \rho_g g\left(h_1 + h_w \sin\theta\right)$$

in which h_w is the difference in water column heights measured in the reclined plane. Pressures P_3 and P_0 are also related as

$$P_3 = P_0 + \rho_w g h_w$$

in which ρ_w is the density of water. Combining equations 10, 11, and 12 gives

$$P_2 - P_1 = g\left(\rho_w - \rho_g\right)h_w \sin\theta \cong g\rho_w h_w \sin\theta$$

because $\rho_w >> \rho_g$. Combining equations 10 and 13, we obtain

$$u_g = \sqrt{\frac{2\rho_w g h_w \sin\theta}{\rho_g}}$$

Note that $u_g \propto \sqrt{h_w \sin\theta}$. Differentiating equation 14 and dividing both sides by u_g yields

$$\frac{du_g}{u_g} = \frac{dh_w}{2h_w}$$

That is, the Pitot probe/manometer sensitivity S_m (defined as dh_w/du_g) is given by

$$S_m \equiv \frac{dh_w}{du_g} = \frac{2h_w}{u_g} \propto \frac{u_g}{\sin\theta}$$

Equation 16 states that S_m vanishes for small velocities and, for a given u_g, increases as q becomes small. That is, for the same u_g, the ratio of $S_m(\theta)$ for a reclining ($0° < \theta < 90°$) manometer and for a normal ($\theta = 90°$) manometer is given by

$$\left.\frac{S_m(\theta)}{S_m(90°)}\right|_{u_g} = \frac{1}{\sin\theta}$$

which for $\theta = 30°$ as used in the present setup gives a "gain" of 2.

When calculating the velocity from the manometer readings, you may use the following values:

$\rho_g = 1.2$ kg/m3 (at 25°C); $\rho_w = 1.0 \times 10^3$ kg/m3; and $g = 9.80$ m/s2.

Note that to limit the velocity error to 1%, we should really know the air temperature and pressure quite accurately. Specifically, from equation 14 and the gas law $p = \rho RT$, we can see that both air temperature and pressure must be known to within 1%. (As may be inferred from equation 14, a 1% error in each of the two quantities introduces individually a 0.5% error in ρ_g; together they appear as a 1% error in u_g.) For example, at near room temperature (~300K), u_g is off by 1% from the above value if the air temperature differs by 3° C from 25° C.

B. Hot Film Anemometer

The hot film anemometer probe operates on the basis of heat transfer. The anemometer electronics keep the film resistance constant by maintaining the film temperature constant. The film temperature is kept constant by controlling the electric current through the film so that joule heating balances gas cooling. Thus, when a hot film sensor is convectively cooled by a stream of moving gas, the electric current through the film is increased to match the cooling. The voltage across the film element, V_f, which is directly related to probe output, V_{out}, thus can be used to indicated flow velocity. To relate quantitatively V_f to flow velocity, we use an empirical heat transfer law for the sensor element:

$$\frac{V_f^2}{R} = \left(A + B\sqrt{u_g}\right)\left(T - T_g\right)$$

where the left-hand side expresses electric heating in the sensor element and the right-hand side expresses gas cooling. R is sensor resistance and T is sensor temperature, u_g is gas velocity, and T_g is gas temperature. A and B are empirical constants. Because T is kept constant, R is also constant, and equation 18 my be expressed as

$$V_f^2 = C + D\sqrt{u_g}$$

Since $Vout$ is proportional to V_f, equation 19 implies that V_f^2 is also related linearly to $\sqrt{u_g}$.

NO. OF
COPIES ORGANIZATION

* ADMINISTRATOR
DEFENSE TECHNICAL INFO CTR
ATTN DTIC OCA
8725 JOHN J KINGMAN RD STE 0944
FT BELVOIR VA 22060-6218
*pdf file only

1 DIRECTOR
US ARMY RSCH LABORATORY
ATTN AMSRD ARL CI IS R REC MGMT
2800 POWDER MILL RD
ADELPHI MD 20783-1197

1 DIRECTOR
US ARMY RSCH LABORATORY
ATTN AMSRD ARL CI OK TECH LIB
2800 POWDER MILL RD
ADELPHI MD 20783-1197

1 DIRECTOR
US ARMY RSCH LABORATORY
ATTN AMSRD ARL D D SMITH
2800 POWDER MILL RD
ADELPHI MD 20783-1197

4 DIRECTOR
US ARMY RSCH LABORATORY
ATTN AMSRD ARL SE RL M DUBEY
B PIEKARSKI
AMSRD ARL SE RM H WALLACE
AMSRD ARL SE SS LADAS
2800 POWDER MILL RD
ADELPHI MD 20783-1197

1 CDR US ARMY TACOM ARDEC
ATTN AMSTA AR FSP M HOLLIS
PICATINNY ARSENAL NJ 07806-5000

1 CDR NAVAL SURF WARFARE CTR
ATTN G33 D HAGEN
17320 DAHLGREN ROAD
DAHLGREN VA 22448-5100

3 PROGRAM MGR ITTS
STRICOM
ATTN AMFTI EL D SCHNEIDER
12350 RESEARCH PKWY
ORLANDO FL 32826-3276

1 US ARMY CECOM RDEC
ATTN AMSEL RD NV AS UEA
G KLAUBER
10221 BURBECK ROAD
FORT BELVOIR VA 22060-5806

NO. OF
COPIES ORGANIZATION

4 APPLIED PHYSICS LABORATORY
ATTN W D'AMICO
11100 JOHNS HOPKINS ROAD
LAUREL MD 20723-6099

ABERDEEN PROVING GROUND

2 DIRECTOR
US ARMY RSCH LABORATORY
ATTN AMSRD ARL CI OK (TECH LIB)
BLDG 305 APG AA

1 CDR USA AMSAA
ATTN AMXSY EF S MCKEY
BLDG 392

1 US ARMY EVALUATION CMD
ATTN USA CSTE EAC AZ R MIRABELLE
BLDG 4120

2 CDR US ARMAMENT RD&E CTR
ATTN AMSTA AR FST T J MATTS
J WHITESIDE
BLDG 120

1 CDR USA DTC
ATTN CSTE DTC TTM J SCHNELL
RYAN BLDG

3 DIR USARL
ATTN AMSRD ARL WM J SMITH
A HORST
AMSRD ARL WM SG T ROSENBERGER
BLDG 4600

2 DIR USARL
ATTN AMSRD ARL WM B D LYON
W CIEPIELLA
BLDG 4600

20 DIR USARL
ATTN AMSRD ARL WM BA T BROWN (2 CYS)
F BRANDON T BROSSEAU
B DAVIS T HARKINS
D HEPNER G KATULKA
R MCGEE P MULLER
P PEREGINO A THOMPSON
M WILSON M CHILDERS (4 CYS)
K HUBBARD
BLDG 4600

NO. OF
COPIES ORGANIZATION

5 DIR USARL
ATTN AMSRD ARL WM BC P PLOSTINS
M BUNDY J GARNER
B GUIDOS J NEWILL
P PLOSTINS
BLDG 390

3 DIR USARL
ATTN AMSRD ARL WM BF
D WILKERSON H EDGE T HAUG
BLDG 390

2 DIR USARL
ATTN AMSRD ARL WM RP J BORNSTEIN
C SHOEMAKER
BLDG 1121